Journal of Building Engineering 76 (2023) 107131

Contents lists available at ScienceDirect

Journal of Building Engineering

journal homepage: www.elsevier.com/locate/jobe

The ambient and elevated temperature performance of hemp fibre reinforced alkali-activated cement foam: Effects of fibre dosage and alkali treatment

K. Dhasindrakrishna [a,b,*], Kirubajiny Pasupathy [b], Sayanthan Ramakrishnan [a], Jay Sanjayan [a]

[a] Centre for Sustainable Infrastructure and Digital Construction, School of Engineering, Swinburne University of Technology, Hawthorn, Victoria, 3122, Australia
[b] Centre for Future Materials, School of Engineering, University of Southern Queensland, Springfield, QLD, 4300, Australia

ARTICLE INFO

Keywords:
Alkali-activated cement
Lightweight binder
Fire resistance
Drying shrinkage
Aerated binder

ABSTRACT

Hemp fibre is gaining attention as a sustainable alternative to synthetic fibres in cementitious composites. This study investigates the effects of dosage and alkali treatment of hemp fibre (HF) on the strength, shrinkage, and fire resistance of alkali-activated cement foam (AACF). Raw untreated and NaOH-treated HFs were added at 0.3%, 0.7%, and 1% of the volume of precursor slurry. The findings reveal that alkali-treated HF increases the compressive strength, which increased with dosage up to 0.7% and then dropped slightly at 1%. Whereas raw HF lowered compressive strength except for 0.7%. Flexural strength was enhanced by both treated and untreated fibre, which increased with the dosage up to 0.7% and then dropped slightly at 1%. The flexural strength enhancement (up to 260%) was higher than compressive strength (up to 54%) at all dosages. Moreover, alkali-treated HF exhibited higher strength compared to raw HF (54% vs 32% under compression and 260% vs 220% under flexure). Residual compressive strength after exposure was measured as an indicator of fire resistance. It followed a similar variation with fibre dosage to their ambient compressive strength when exposed to 100°C and 200°C, where the optimum dosage of 0.7% had up to 65% higher strength for treated fibre and 16% higher strength for raw fibre. However, HF did not improve the residual strength for higher temperatures (400°C and 800°C). In contrast, they caused a higher proportion of strength loss by up to 83–91% of the original strength compared to 67–84% in the control.

1. Introduction

Foam concrete is a type of porous concrete prepared by artificially introducing voids in cement paste or mortar through a suitable foaming method. They remain a popular lightweight construction material because of their lower thermal conductivity, improved fire resistance and reduced self-weight. In general, Ordinary Portland cement (OPC) is used as the binder to produce this conventional foam concrete. However, due to the rising concerns over the greenhouse gas emission (GHG) associated with OPC and its increasing demand, alkali-activated cements (AAC) are being explored as a substitute for OPC in foam concrete [1]. The replacement of OPC with AAC can reduce the GHG emissions associated with concrete by up to 80% [2].

* Corresponding author. Centre for Future Materials, School of Engineering, University of Southern Queensland, Springfield, QLD, 4300, Australia.
E-mail address: Dhasindrakrishna.Kitnasamy@usq.edu.au (K. Dhasindrakrishna).

https://doi.org/10.1016/j.jobe.2023.107131
Received 17 February 2023; Received in revised form 14 June 2023; Accepted 16 June 2023
Available online 17 June 2023

The porous structure of alkali-activated cement foam (AACF) results in enhanced thermal insulation like the OPC-based foam concrete. In addition, AACFs produced from low calcium precursors like class F fly ash (also known as geopolymers) can provide superior fire resistance due to their polymer structure [1]. However, AACFs possess lower strength and display higher shrinkage similar to their OPC counterpart [1,3]. Therefore, flexible fibres like polyvinyl alcohol (PVA), polypropylene (PP) and basalt are generally used to improve these properties [4–7]. These fibres strongly adhere to the AAC through chemical and frictional bonds at the surface. Through these bonds, they bridge across the cracks formed under a load and resist the growth of cracks, improving the overall strength of the composite [8–10]. Especially in AACF, fibres can also improve mechanical performance by reducing the fluidity of the fresh AAC slurry in addition to the fibre-bridging action in hardened AACFs. In the fresh AAC slurry, fibres impose a resistance to flow because of their interlocking behaviour and reduce the slurry's fluidity. This can result in finer pores in the AACF and increase overall strength [11]. The fibre bridging action can also improve durability by reducing drying shrinkage [9,12]. Also, these fibres melt when the fibre-reinforced AACF is exposed to fire, resulting in voids. These voids will act as pathways for the water vapour to escape and prevent the AACF from failing (cracking, spalling or disintegrating) due to excessive vapour pressure [4].

Having established the vital role of fibres in foam concretes and AACF, current efforts can be seen to replace these synthetic fibres with plant-based natural fibres (such as hemp, jute and kenaf), which are more sustainable, less toxic, widely available and cost-effective [13]. Among these fibres, hemp has received relatively higher attention because of its shorter maturity time (3.5 months), higher carbon storage potential and higher tensile strength [10,14]. Natural fibres are mainly composed of cellulose, hemicellulose and lignin polymer chains [15,16]. Here, the cellulose, because of its crystalline structure, is the stiffest and strongest component providing strength, stiffness and stability to the fibre. Hemp is made of around 80% cellulose by weight which is a relatively higher range among plant-based fibres [16].

A considerable body of research has already been reported on hemp-based cementitious composites. They show that incorporating hemp fibre improves mechanical properties and reduces drying shrinkage in OPC and AAC-based mortars [17–20], where the extent of these improvements depends on fibre composition and fibre-AAC interfacial bond [18]. Raw hemp fibre has hence been generally pre-treated following various procedures to improve the fibre composition and interfacial bond, among which alkali treatment using NaOH can be found as the commonly followed procedure. This process removes the non-cellulosic components (such as hemicellulose and lignin) and impurities (such as waxes and oils), which are detrimental to the performance of the resultant composite. First, these components degrade in an alkali medium, affecting the durability of fibres and thereby undermining the composite's properties over time [15,16,18,21–23]. Also, because of their hydrophobic nature, these components reduce the adhesion between the fibre and the hydrophilic AAC matrix, which in turn negatively affects the mechanical properties [24]. Additionally, hemicellulose, in particular, retards the alkali activation reaction [15]. Therefore, their removal from pre-treatment is beneficial to the overall performance of the composite. As mentioned before, cellulose is the primary component that gives the fibre its strength [16]. Also, cellulose bonds well with the AAC matrix [15]. Therefore, the removal of other components increases the cellulose content in the fibre, which improves the strength of individual fibre and that of the resultant composite [25,26]. The NaOH treatment also defibrillates the fibre and creates a rougher surface, improving the bonding between the fibre and AAC/cement matrix [19,27].

Such observations of improved composite properties with alkali treatment are consistent for hemp fibre in cement matrix [27]. However, contradicting results have also been reported for AACs, where the alkali treatment has degraded the composites' performance in a few studies [10,19,21]. This was attributed to the strong alkaline environment used to produce AACs, where a pre-treated fibre might expose the cellulose chains to further alkali attack. This affects its crystallinity and thereby lowers the strength of individual fibres and the resultant AAC composite [20,26]. Whereas, in an untreated fibre, this strong alkali medium will remove the non-cellulosic components similar to the regular pre-treatment procedure, referred to as self-treatment [10,21]. Meanwhile, it should be noted that these conflicting observations could be a result of the different alkali treatment procedures followed in those works. Therefore, finding the effective alkali-treatment conditions for AAC composites requires further understanding in terms of concentration, duration, and temperature.

Regarding the thermal performance of hemp fibre, their thermal degradation is caused by the decomposition of cellulose, hemicellulose and lignin polymer chains under heat. As in the mechanical strength, the cellulose chains contribute greatly to fire resistance because of their crystalline structure. Therefore, the alkali treatment improves the thermal stability of hemp fibre by increasing the cellulose content [28,29]. However, the influence of hemp fibre and alkali treatment on the residual properties of the resultant composite after heat exposure is not widely reported.

Despite the considerable amount of work available on hemp fibre-based composites, the effects of hemp fibre on AACFs remain largely unexplored. Recently, Gencel et al. [30] have reported the benefits of hemp fibre in OPC-based foam concrete such as improved strength (compressive and flexural) and reduced drying shrinkage. However, as mentioned above, the interaction between the fibre and AAC and their durability in the AAC matrix are different due to the highly alkaline environment. Also, AACs exhibit a different response to heat and drying shrinkage depending on the precursor. Therefore, understanding the effects of hemp fibre in AACFs requires experimental investigation. To the authors' best knowledge there are no available studies that have assessed the effects of hemp fibre on AACFs.

Here, we assess the influence of hemp fibre on the strength, elevated temperature performance and drying shrinkage of AACF. They are assessed at different fibre dosages separately for alkali-treated and raw hemp fibre to understand the effect of fibre dosage and alkali treatment. The efficiency of the selected treatment process was verified through scanning electron microscopy (SEM). The effect of fibre on the rheology of AAC slurry was investigated and correlated with the hardened properties.

2. Materials and methods

2.1. Materials

A combination of Ground Granulated Blast-furnace Slag (hereafter referred to as slag) and fly ash at a ratio of 70:30 was used as the precursor to prepare the AAC slurry. The slag and fly ash were obtained from Independent Cement and Lime Pty Ltd., Australia and Cement Australia, respectively. The precursors were activated using sodium hydroxide (>98% NaOH by weight) and anhydrous sodium metasilicate (50–51.5% Na_2O and 45.5–47.5% SiO_2 by weight). Both sodium hydroxide and sodium metasilicate were purchased from Redox Pty Ltd, Australia. Glucopon® 225 DK, a non-ionic surfactant provided by BASF Australia Ltd., was used as the foaming agent. The hemp fibre was obtained from a local supplier, and its specific gravity was determined as 1.23 ± 0.03. The thickness of individual hemp fibre measured from SEM images varied from 15 μm to 80 μm depending on the degree of bundling. The alkali treatment was performed by immersing the hemp fibre in 1.63 M NaOH solution for 1 h at 95°C. Once removed from the NaOH solution, they were washed thoroughly and dried at 70°C for 12 h. The hemp fibre was manually cut into small pieces approximately 10 mm in length before being added to the AAC slurry.

2.2. Sample preparation

Seven sets of AACF specimens were prepared for this study. It consisted of three different hemp fibre dosages for both treated and untreated fibre and a control mix without fibre. The mix compositions given as weight percentages are summarised in Table 1. Mix 1 represents the control AACF mix without any fibre. Mix 2, Mix 3 and Mix 4 respectively represent the AACF with 0.3%, 0.7% and 1% hemp fibre by volume of the AAC slurry used for aeration. 0.3%, 0.7% and 1% of fibre to the volume of precursor slurry correspond to 0.15%, 0.36% and 0.51% of fibre to the weight of the total ingredients given in Table 1. The corresponding AACFs with the alkali-treated hemp fibre are denoted by the Mix name followed by T inside the parenthesis, e.g., Mix 2 (T).

The activating solution was prepared by sequentially dissolving the sodium silicate and sodium hydroxide pellets in warm water (60°C) before beginning the mixing process. The resultant solution was then allowed to cool down to room temperature (≈22°C). The AACF was prepared through mechanical foaming, where the AAC slurry and the premade foam were prepared separately and mixed in the next step. To prepare the AAC slurry, the precursors were first mixed for 2 min in a Hobart planetary mixer at slow speed to obtain a homogenous dry mixture. Then, the activator solution was added to the dry mixture and mixed for another minute at an intermediate speed. Following this, the hemp fibre was added to the wet mixture and mixed well for 2 more min at a higher speed. The aqueous foam was prepared by mixing the diluted foaming agent (1 part of Glucopon in 100 parts of water) using a high-shear mixer rotating at 2000 rpm for about 5 min. The required amount of aqueous foam and the AAC slurry were then mixed using the Hobart planetary mixer at a slower speed for 3 min–5 min until a uniformly distributed bubble slurry system was achieved. Finally, the fresh AACF was cast in 50 x 50 × 50 mm^3 cubic mould and 40 x 40 × 160 mm^3 prism moulds and cured at 25°C and 50% RH for 24 h inside an environmental chamber to obtain the hardened AACF specimens. These hardened specimens were then sealed and cured inside the same environmental chamber (25°C and 50% RH) until the 28th day.

2.3. Testing methods

2.3.1. Mechanical strength

The compressive strengths of the hardened specimens were measured using an Instron-5965 universal mechanical testing machine at a displacement rate of 2 mm/min after 28 days of curing. Three 50 × 50 × 50 mm^3 cubic samples were tested for each AACF mix and the average was considered for analysis. The specific compressive strengths were obtained by dividing the average compressive strengths by corresponding average densities. Here, the densities were calculated from the volume (obtained from linear measurements) and weight of the specimens.

Flexural strengths were tested on the 40 x 40 × 160 mm^3 prism specimens supported symmetrically at a spacing of 120 mm and loaded at the centre as described in ASTM C348-21 [31]. A loading rate of 1 mm/min was adopted. The flexural strength (Sf in MPa) was calculated from the ultimate load (P in N) using the relationship given in ASTM C348-21 (Eq. (1)) [31]. Like the compressive strength test, three specimens were tested for each AACF mix and the average value was considered.

$$Sf = 0.0028 \text{ x } P \tag{1}$$

2.3.2. Fire resistance

Fire resistance was assessed through the residual strength of the AACF specimens after exposing them to selected elevated temperatures following the procedure described in existing literature [32,33]. The selected exposure temperatures were 100°C, 200°C,

Table 1
Mix design given as weight percentages (%).

	Mix 1	Mix 2	Mix 3	Mix 4
Slag	38.71	38.65	38.57	38.51
Fly ash	16.59	16.56	16.53	16.51
Water	30.41	30.37	30.31	30.26
Sodium silicate	5.53	5.52	5.51	5.50
Sodium hydroxide	2.76	2.76	2.76	2.75
Foam	5.99	5.98	5.97	5.96
Hemp fibre	0.00	0.15	0.36	0.51

400°C and 800°C. The specimens were heated inside a muffle furnace to the target temperature and were soaked in this temperature for 1 h. They were then allowed to cool down to room temperature for strength measurements. Three 50 x 50 × 50 mm^3 cubic specimens, cured for 28 days, were used for each exposure temperature and the residual compressive strength was determined as described in section 2.3.1.

2.3.3. Drying shrinkage

Drying shrinkage was measured on 40 x 40 × 160 mm^3 prism specimens following the recommendations given for autoclaved aerated concrete in RILEM-ACC 5.1 1992 [3,34]. Spherical gauge plugs were attached to the ends of the specimens and the length measurements were taken using a Vernier calliper (accuracy = 0.01 mm > 0.03% of the specimen's length). Three specimens were used for each mix and the average values are reported here. The first length measurement was taken after curing the specimens for 7 days under sealed conditions. Repeated measurements were taken until at least 56 days while keeping the specimens exposed at 25°C and 50% relative humidity.

2.3.4. Micromorphology analysis of fibre

The morphology of raw and alkali-treated hemp fibre was observed using a scanning Electron Microscope (SEM, ZEISS Supra 40 V P) to examine the effects of alkali treatment. Before conducting the test, the fibre was gold coated to a thickness of 15 nm using a K975X vacuum coating system.

2.3.5. Flow measurement

The effect of fibre on the rheology of the AAC slurry used for mechanical foaming was studied using a mini-cone following the ASTM C1437-07 standard [35]. The AAC slurry without the foam (prepared as described in section 2.2) was filled inside the flow cone in two layers and tamped 20 times with a tamper after filling each layer. Then the mould was lifted, and the table was dropped 25 times to obtain the flow diameter.

3. Results and discussion

3.1. Effects of alkali treatment on the morphology of hemp fibre

A wide range of alkali treatments have so far been reported for hemp fibre with varying NaOH concentration, soaking duration and temperature. Therefore, SEM images of the fibre were first analysed to verify the efficiency of the alkali treatment adopted in this work. Fig. 1 shows that the untreated fibre is bundled and had dirt-like substances on the surface. The binding components are hemi-celluloses, lignin, pectin and other substances. Whereas the dirt-like substances could be impurities such as wax and oils [26]. The alkali treatment unpacked the fibre bundle to expose individual fibres and the groves between them. This showed the adopted alkali treatment effectively removed hemicelluloses, lignin, pectin, wax and oils. This removal of impurities must increase the proportion of cellulose to the total mass of fibre, which can increase its strength. The improved fibrillation and well-defined grooves should help bonding between the fibre and the AAC matrix [26]. Also, pectin can trap calcium and inhibit the growth of C–S–H hydrates (the resultant product from the alkali activation of slag), and the removal of pectin should improve the extent of alkali activation compared to untreated fibre [27].

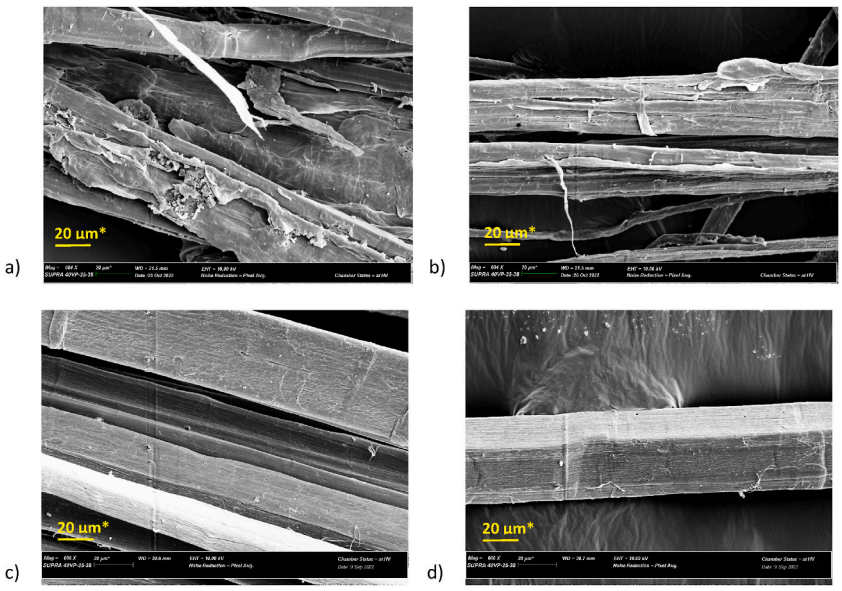

Fig. 1. SEM images of hemp fibre: (a and b) – Untreated raw fibre and (c and d)- Alkali treated fibre
*The original scale is in the ribbon at the bottom of the image. However, it is manually drawn in larger size here for clarity.

3.2. The effect of fibre on the rheology of fresh AAC slurry

Assessing the influence of fibre on the rheology of AAC slurry used for foaming is important as it may affect the pore characteristics of the hardened AACF, which will consequently affect mechanical strength and fire performance [1]. Fibres, in general, pose a resistance to flow and reduce the fluidity in cementitious pastes. In addition, hemp fibre should absorb water due to its hygroscopic nature and further reduce the flowability [30]. This should have resulted in reduced flow diameter with fibre content. However, from Fig. 2, we can see that the fibre had a negligible effect on the flow diameter. The diameter of the control mix was 175 mm, and the highest and lowest spread diameters were 182 mm and 162.5 mm obtained for Mix 2 (T) and Mix 4 (T), respectively. This showed a change in the range between +7 mm and −12.5 mm. Also, this change did not follow any trends with the fibre dosage. Meanwhile, the studied AAC had a higher proportion of slag in the precursor and sodium silicate as an activator. This combination results in rapid yield stress growth due to the formation of primary C–S–H gel through the reaction between Ca^{2+} from slag and silicate ions [36]. Therefore, we can say that the faster yield stress development in the AAC slurry, in this case, should have outweighed the effects of hemp fibre on the rheology. This should also be partly attributed to the test procedure, where the fresh slurry is allowed to rest inside the mini cone for 1 min. This gave enough time for a rapid yield stress gain in the AAC which could have overshadowed the effects of hemp fibre. Even though the table is dropped after this, the relevant shear stress might not be enough.

3.3. Mechanical properties

3.3.1. Compressive strength

Adding fibres to a cementitious system has two inherent effects that can either improve or degrade the mechanical properties of the resultant composite. The positive effect is the fibre-bridging action, where the fibres bridge across cracks and resist crack propagation through chemical and frictional bonds with the cement matrix [8]. This will enhance the composite's resistance to failure and its load-bearing capacity. The adverse effect is the defects caused by the addition of fibres such as cavities and fibre clusters, which results in poor fibre bonding that weakens the cementitious matrix and reduces the overall strength of the composite [37]. Also, since fibre is weak in compression, the solid volume which can resist compression decreases as the fibre volume increases, which affects the compressive strength of the composite [38]. The resultant effect varies according to the type and dosage of fibre. In foam concretes, fibres might also indirectly affect mechanical properties by modifying the pore characteristics through their effect on rheology. However, since the hemp fibre did not significantly affect the rheology of the studied AAC slurry in the considered dosage (section 3.2), we can attribute the observed variation of mechanical properties (Fig. 3) to fibre bridging action and defects associated with the addition of hemp fibre. The impact of these two effects on the resultant mechanical performance has however varied with the fibre treatment process, dosage and type of loading.

According to Fig. 3, considering the addition of untreated fibre, the compressive strength at 0.3% and 1% fibre dosages (Mix 2 and Mix 4) were lower than the control mix (Mix 1). The highest compressive strength was obtained for an intermediate fibre dosage of 0.7% in Mix 3. The compressive strength variation among samples reinforced with alkali-treated hemp fibre also showed a similar trend, i.e., a peak compressive strength at 0.7% dosage. However, the compressive strengths of the samples reinforced with alkali-treated hemp fibre were always higher than the control sample. Also, for a given dosage, the alkali-treated fibre resulted in a higher compressive strength than the untreated fibre.

We observed a slight variation in density among the samples despite the same foam content (Fig. 3b). This can be attributed to the sensitivity of the mixing procedure. In some of these samples, their densities complemented strength. For instance, the higher density of Mix 3 compared to Mixes 1, 2 and 4 agreed with its higher strength. Similarly, the higher density of Mix 3 (T) compared to Mix 1, 2 (T), and 4 (T) complemented its higher strength. On the contrary, Mix 4 (T) despite having a lower density than Mix 4, Mix 1 and Mix 2,

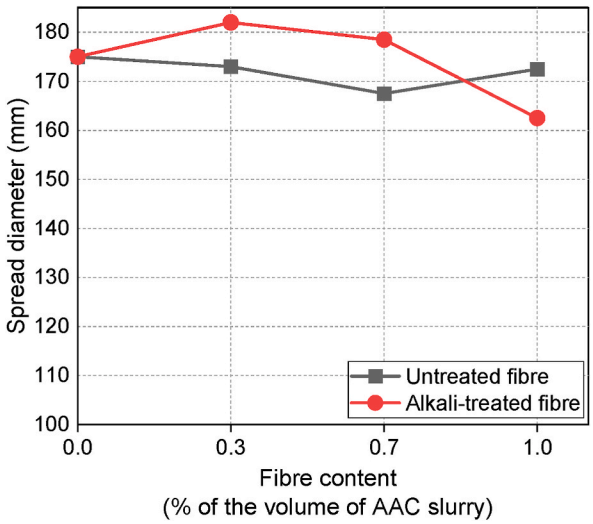

Fig. 2. Variation of flow diameter of the AAC slurry with fibre dosage.

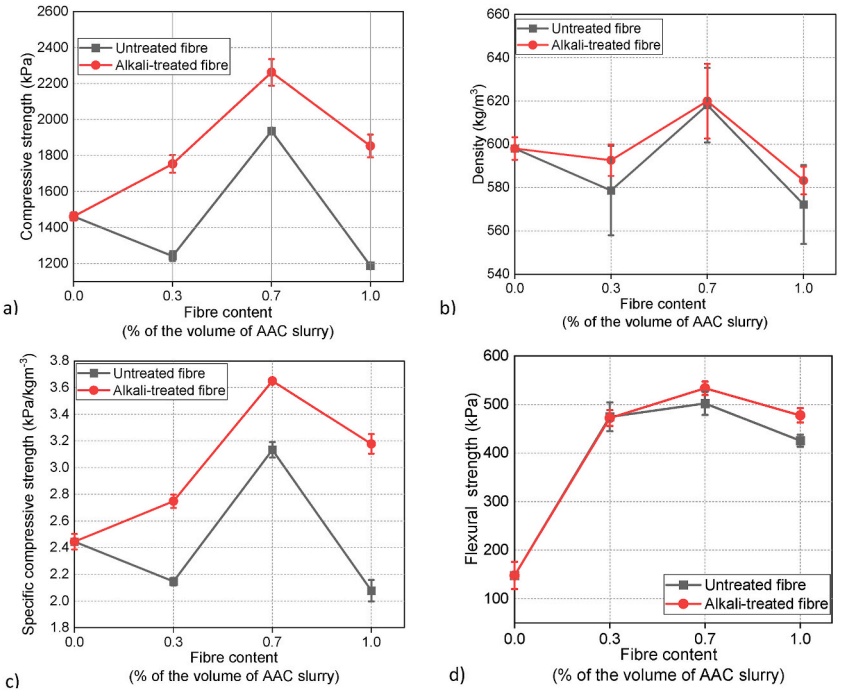

Fig. 3. Variation of mechanical properties with fibre dosage for treated and untreated fibre: a) Compressive strength, b) density, c) Specific compressive strength and d) Flexural strength (The error bars represent one standard deviation from the average values).

possessed a higher compressive strength. This suggests that this variation in compressive strength cannot be completely attributed to the influence of fibre. Therefore, to eliminate the influence of density on compressive strength, specific compressive strengths were considered for further analysis (Fig. 3c). The specific compressive strength also followed a similar trend as the compressive strength with fibre dosage and treatment process.

Considering the specific compressive strength of samples reinforced with untreated hemp fibre, we can notice that the defects caused by fibre outweighed the merits of fibre bridging at 0.3% (Mix 2) and 1% (Mix 4) dosages. At the optimum dosage of 0.7% in Mix 3, the benefits of fibre bridging had the dominant effect, resulting in a higher compressive strength than the control sample. On the other hand, samples reinforced with alkali-treated hemp fibre always showed a higher specific compressive strength than the control specimen. This indicates that the fibre bridging action outweighed the associated defects in AACF reinforced with alkali-treated hemp fibre regardless of dosage. But they also showed a similar trend with 0.7% being the optimum dosage (Mix 3 (T)), which showed there is still a variation in the balance between fibre bridging and defects with the dosage. Also, at any given dosage, the AACF samples reinforced with alkali-treated hemp fibre showed a higher specific compressive strength than that reinforced with untreated hemp fibre. This could be attributed to various advantages of alkali treatment such as the removal of hydrophobic contaminants (e.g., wax and oils), increase in cellulose content and increased surface area due to defibrillation. This should have improved the strength of individual fibres and the fibre–AAC bonding.

3.3.2. Flexural strength

Unlike the compressive strength, which reduced with fibre integration for some dosages (in Mix 2 and Mix 4 with 0.3% and 0.7% untreated fibre, respectively), the flexural strength always increased with the addition of hemp fibre compared to the control sample (Fig. 3d). Also, the magnitude of this strength enhancement was much higher than compressive strength. For instance, the alkali-treated fibre increased flexural strength by 260% at the optimum dosage of 0.7%, whereas the corresponding compressive strength gain was only 54%. This large improvement of load-carrying capacity under flexure compared to that under compression can be attributed to the higher tensile capacity of hemp fibre. Fibres are very weak under compression [38]; therefore, the only mechanism through which they improve compressive strength is by resisting crack propagation [8]. On the other hand, fibres have a very high tensile capacity compared to the AAC matrix, which can improve flexural strength by directly carrying the flexural load in addition to resisting crack propagation.

The variation of flexural strength still showed a few similarities to the variation of compressive strength with dosage and treatment process. For example, the maximum flexural strength was obtained for an optimum dosage of 0.7% and the AACFs reinforced with alkali-treated fibre showed higher strength than those reinforced with untreated fibre. This can also be attributed to the balance between fibre-bridging and defects induced by fibre reaching an optimum point at 0.7% dosage and the benefits of alkali pretreatment of fibre.

3.4. Shrinkage

The AACF samples showed severe shrinkage ranging between 1×10^{-2} mm/mm and 1.2×10^{-2} mm/mm at the end of testing as shown in Fig. 4. This higher shrinkage can be a result of using slag as the major precursor and the absence of coarse aggregates [3,39]. Because of the higher proportion of slag in the precursor, the resultant AAC is dominated by C–S–H gel as in alkali-activated slag (AAS) [40]. AAS generally suffers severe shrinkage due to a combined effect of higher drying and autogenous shrinkages [41]. This shrinkage is further worsened by the absence of coarse aggregates (the studied AACF does not contain fine aggregates as well), which is a common issue in aerated concretes [3].

The drying shrinkage of AACF reduced with the incorporation of both treated and untreated hemp fibre as seen in Fig. 4. Also, the control sample developed severe cracks with time, which was absent in the fibre reinforced AACF samples (Fig. 5). Similar observations of reduced drying shrinkage with the inclusion of flexible fibres (synthetic and natural) can be found in the literature [9,42]. However, the underlying mechanisms are not yet clear. The possible reason for such behaviour can either be the resistance imposed by fibre to dimensional changes from drying (fibre-bridging action) [5,9,43] or the slower rate of drying because of the moisture retained by the fibre [42,44,45].

From the variation of mechanical properties with fibre dosage, we can see that maximum fibre bridging was obtained at 0.7% dosage for both treated and untreated fibre. However, the extent of drying shrinkage continuously reduced with the fibre dosage. Also, the mechanical strength results showed that alkali treatment enhanced the fibre bridging. But the shrinkage in these samples did not vary much with the alkali treatment. From this, we can say the reduced drying shrinkage with fibre is not completely because of the fibre bridging the cracks and resisting movements. On the other hand, the mass change in these samples reveals that the addition of hemp fibre lowers moisture loss (Fig. 4 - c and d), complementing the variation of drying shrinkage. Hemp fibre is hygroscopic due to the presence of hydroxyl groups in the cellulose chains, to which the water molecules stay linked through hydrogen bonds [42,44,46]. Also, the porous structure and the presence of lignin, pectin, wax and nitrogen-containing substances improve the water adsorption capacity of hemp fibre [47]. Therefore, from the reduced rate of mass loss with fibre dosage and the hygroscopic nature of hemp fibre, we can say the lower drying shrinkage in fibre-reinforced AACF agrees more with the lower rate of drying compared to fibre bridging [42,44,45]. By comparing this behaviour with the effects of superabsorbent polymers on the drying of cement-based mortars studied in the past [48], two interesting parallels can be drawn regarding how the water-retaining ability of hemp fibre could have reduced the drying rate: 1. Reduced effective water content – since the fibre absorbs a lot of water, it lowers the amount of water which becomes a part of the binder and contributes to drying shrinkage and 2. Higher internal relative humidity – because of the water retained by the fibre, the internal relative humidity of the samples must be higher, consequently lowering both autogenous and drying shrinkages [48,49].

Even though hemp fibre mitigated drying shrinkage in this study, it should be acknowledged that similar natural fibres have also been reported to increase the drying shrinkage in fibre-reinforced cementitious composites. In such cases, the porous structure of

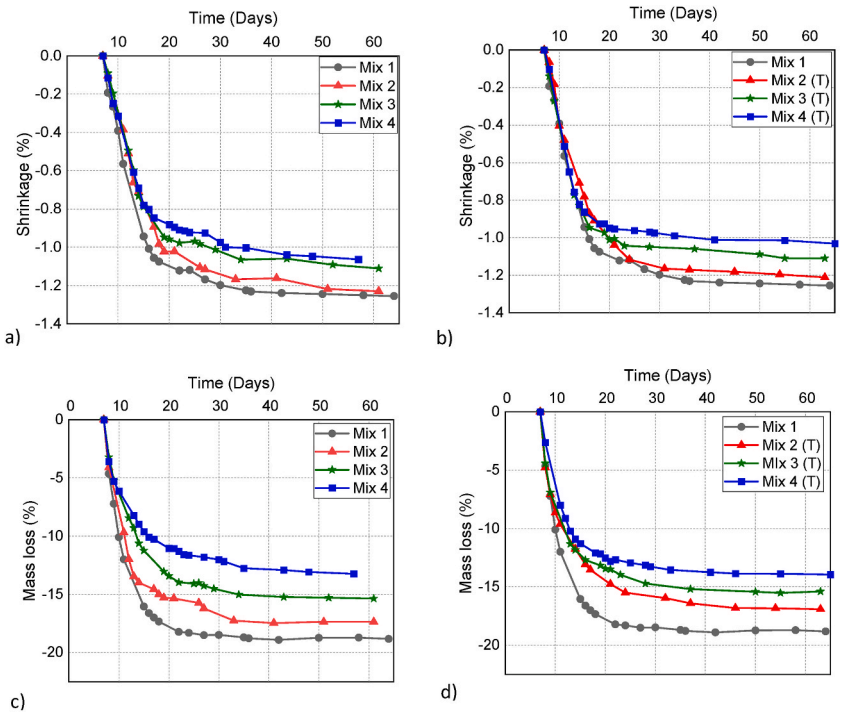

Fig. 4. Variation of drying shrinkage and mass with time: a) Drying shrinkage and c) Mass change in AACF reinforced with untreated fibre and b) Drying shrinkage and d) Mass change in AACF reinforced with alkali-treated fibre.

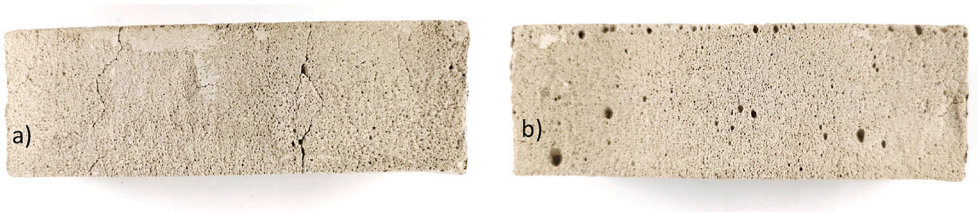

Fig. 5. Drying shrinkage samples at the end of testing: a) Control sample -Mix 1 and b) Example of a fibre-reinforced sample - Mix 2 (T).

natural fibres, which is considered to make the fibre hygroscopic and lower the drying shrinkage, has also been said to accelerate moisture loss by forming pathways for moisture movement [43,50,51]. This shows that the effects of natural fibres on the drying shrinkage of OPC and/or AAC-based composites are not conclusive and require more evidence and explanations.

3.5. Fire resistance

The strength of AACF samples exposed to elevated temperatures was always lower than the unexposed samples and reduced with the exposure temperature as shown in Fig. 6 (a and b). This strength loss can be attributed to the presence of slag as the major precursor. AAS generally loses its strength at elevated temperatures due to the removal of water which results in thermal contraction and microcracks [52,53]. This thermal contraction and microcracking are severe between 100°C and 200°C due to the removal of physically bound water. This explains the rapid strength loss up to 200°C, which did not decrease much when further heated to 400°C and 800°C [52,53].

Looking at the residual strength after exposure to 100°C and 200°C (Fig. 6 a and b), it generally followed a similar trend to the ambient compressive strength (Fig. 3a and c); however, there are a few exceptions to this general trend. For instance, the AACF samples reinforced with alkali-treated fibre (except Mix 4(T) at 200°C) showed almost equal or higher residual strength than the control sample with a dosage of 0.7% resulting in the maximum strength (Fig. 6b). This corresponds with the variation of ambient compressive strength with fibre dosage in alkali-treated fibre reinforced AACF (Fig. 3a). A similar agreement can be observed between the ambient compressive strength of AACF samples reinforced with untreated fibre (Fig. 3a) and the residual strength of those exposed to 200°C (Fig. 6 a). Here, a dosage of 0.7% (Mix 3) showed higher residual strength than the control specimen, whereas the other two dosages (0.3% - Mix 2 and 1% - Mix 4) showed a lower residual strength (Fig. 6a). Even though a similar observation can be made for the samples reinforced with untreated fibre exposed to 100°C, the variation is very small. When the exposure temperature was further increased, at 400°C and 800°C, the samples did not show much variation in strength (except Mix 4 and Mix 4 (T) which had the highest

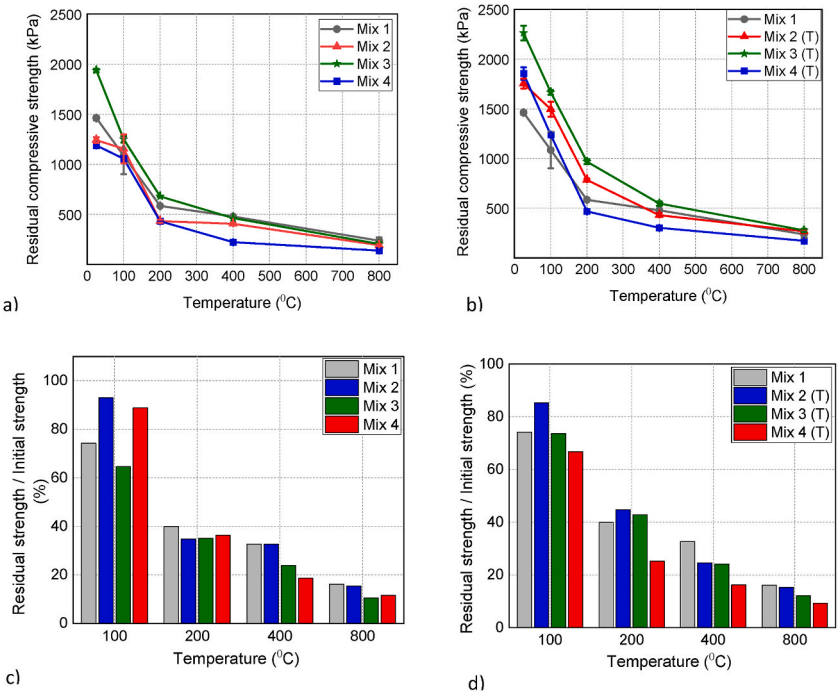

Fig. 6. The residual strengths of AACFs given as strength values (a and b) and percentage of ambient strength (c and d): a) and c) – AACFs reinforced with untreated hemp fibre and b) and d) - AACF reinforced with alkali-treated hemp fibre. (The error bars represent one standard deviation from the average values).

percentage of fibre). Moreover, the control sample generally performed equal to or better than the fibre-reinforced samples at 400°C and 800°C (both untreated and alkali-treated). Therefore, we can observe the presence of two temperature regimes, wherein in the lower temperature regime (100°C and 200°C), the residual strength varied with the fibre content similar to the ambient compressive strength. On the other hand, at the higher temperature regime (400°C and 800°C), the residual strength did not change much with the fibre content. These two regimes agreed with the major thermal decomposition range of hemp fibre 200–400°C [19,25,29].

Considering the first regime, as mentioned above, the residual strength after exposure to 100°C and 200°C followed a similar trend to their ambient strength with the fibre dosage. For these temperatures, Mix 2(T), Mix 3, Mix 3(T) and Mix 4(T) showed a higher residual compressive strength than the control samples (Except Mix 4(T) at 200°C) as seen in Fig. 6(a and b). Despite this improved residual strength, the percentages of respective initial strengths retained by these samples did not follow the same trend (Fig. 6 c and d). For instance, Mix 3, Mix 3 (T) and Mix 4(T), which showed higher residual strength than the control sample when exposed to 100°C, retained only a smaller proportion of their ambient strength compared to the control sample. A similar discrepancy can be observed for Mix 3 at 200°C. Therefore, we can say that, at 100°C and 200°C, the residual strength of the fibre reinforced AACF was directly affected by the presence of hemp fibre similar to how they affected the ambient strength (discussed in section 3.3.1). This is determined by the balance between fibre-bridging action and defects induced by fibre, depending on dosage and pre-treatment. However, the hemp fibre did not minimise the strength loss due to the thermal contraction of the AACF.

In the second regime (400°C and 800°C), because of the thermal decomposition, fibre can no longer have a direct effect on the residual strength. They could still indirectly affect the residual strength through the space left by burnt fibre that act as dehydration pathways and prevent strength loss [4]. However, the retained strength given as a percentage of initial strength has lowered with the fibre dosage at 400°C and 800°C. This could be attributed to the increase in overall porosity from the pores left by burnt fibre [7]. This shows that the pores created by the decomposed hemp fibre is not efficient in preventing strength loss from thermal contraction.

4. Conclusions

This study assesses the effects of hemp fibre on the mechanical and elevated temperature performance of AACF. Three fibre contents of 0.3%, 0.7% and 1% (by the volume of precursor slurry) were considered to identify the effects of dosage. Both untreated and alkali-treated hemp fibre was used to identify the effects of alkali treatment. The following conclusions can be drawn from this study.

- The NaOH pre-treatment with 1.63 M NaOH solution for 1 h at 95°C was found suitable for alkali-activated cement. It efficiently removed the impurities and non-cellulose components and defibrillated the fibre, which enhanced the mechanical properties.
- Alkali-treated hemp fibre enhances the strength of AACF more than raw fibre. The untreated fibre increased the compressive strength only at the optimum dosage of 0.7% (by 32%) and degraded the compressive strength at other dosages (by up to 18%). Meanwhile, the treated fibre consistently increased the compressive strength (by 20–54%). Likewise, the flexural strength increased by 220–260% for treated fibre compared to 188–240% for untreated fibre. The strength enhancement by hemp fibre was much higher under flexure (up to 260%) compared to compression (up to 54%).
- There is an optimum dosage that results in the maximum strength where the benefits of fibre bridging outweigh the defects from fibre by the greatest ratio. Above this dosage, strength starts to drop. This dosage was found as 0.7% for both treated and untreated fibre.
- The AACF displayed high shrinkage in the range of 1.25×10^{-2} mm/mm. Hemp fibre reduced this shrinkage with dosage for both treated and untreated fibre (down to around 1×10^{-2} mm/mm). This behaviour agrees with the ability of fibre to retain water and slow down the drying process.
- Hemp fibre is effective in improving fire resistance at lower exposure temperatures. The AACF reinforced with 0.7% alkali-treated fibre resulted in the highest residual compressive strength which was 53% and 65% higher than the control mix at 100°C and 200°C, respectively. The untreated fibre also resulted in a higher residual strength than the control (by 15–16%) at these temperatures but it was lower than the alkali-treated fibre.
- Hemp fibre is not efficient in improving fire resistance at higher exposure temperatures (at 400°C and 800°C), where the AACF samples did not show a big variation in residual compressive strength with the fibre dosage. Moreover, the proportion of respective initial strength retained after heat exposure decreased with the fibre dosage by up to 83% at 400°C and 91% at 800°C. Whereas, the control AACF lost only around 67% at 400°C and 84% at 800°C. This can be attributed to the increased porosity from the space left by burnt fibre.

Author statement

Dhasindrakrishna Kitnasamy: Conceptualization, Methodology, Formal analysis, Investigation, Writing – Original Draft, Visualization.

Sayanthan Ramakrishnan: Conceptualization, Methodology, Writing – Review & Editing, Visualization, Supervision, Funding acquisition.

Kirubajiny Pasupathy: Conceptualization, Methodology, Writing – Review & Editing, Visualization, Supervision, Project administration.

Jay Sanjayan: Conceptualization, Writing – Review & Editing, Supervision, Project administration, Resources, Funding acquisition.

Declaration of competing interest

The authors declare that they have no known competing financial interests or personal relationships that could have appeared to influence the work reported in this paper.

Data availability

Data will be made available on request.

Acknowledgement

The first author would like to acknowledge the Swinburne University of Technology for supporting this work through the SUPRA scholarship and the DVCR writing award.

References

[1] K. Dhasindrakrishna, et al., Progress, current thinking and challenges in geopolymer foam concrete technology, Cement Concr. Compos. 116 (2021), 103886.
[2] Y.H.M. Amran, et al., Clean production and properties of geopolymer concrete; A review, J. Clean. Prod. 251 (2020), 119679.
[3] E.K.K. Nambiar, K. Ramamurthy, Shrinkage behavior of foam concrete, J. Mater. Civ. Eng. 21 (11) (2009) 631–636.
[4] W.D.A. Rickard, L. Vickers, A. van Riessen, Performance of fibre reinforced, low density metakaolin geopolymers under simulated fire conditions, Appl. Clay Sci. 73 (1) (2013) 71–77.
[5] Z. Abdollahnejad, et al., Comparative Study on the Drying Shrinkage and Mechanical Properties of Geopolymer Foam Concrete Incorporating Different Dosages of Fiber, Sand and Foam Agents, Springer International Publishing, Cham, 2018.
[6] S. Zhang, V.C. Li, G. Ye, Micromechanics-guided development of a slag/fly ash-based strain-hardening geopolymer composite, Cement Concr. Compos. 109 (2020), 103510.
[7] K. Dhasindrakrishna, et al., Rheology and elevated temperature performance of geopolymer foam concrete with varying PVA fibre dosage, Mater. Lett. (2022), 133122.
[8] V.C. Li, A simplified micromechanical model of compressive strength of fiber-reinforced cementitious composites, Cement Concr. Compos. 14 (2) (1992) 131–141.
[9] M. Mastali, et al., Mechanical and acoustic properties of fiber-reinforced alkali-activated slag foam concretes containing lightweight structural aggregates, Construct. Build. Mater. 187 (2018) 371–381.
[10] B. Galzerano, et al., Hemp reinforcement in lightweight geopolymers, J. Compos. Mater. 52 (17) (2018) 2313–2320.
[11] Y. Hao, G. Yang, K. Liang, Development of fly ash and slag based high-strength alkali-activated foam concrete, Cement Concr. Compos. 128 (2022), 104447.
[12] N. Ranjbar, et al., Mechanisms of interfacial bond in steel and polypropylene fiber reinforced geopolymer composites, Compos. Sci. Technol. 122 (2016) 73–81.
[13] M. Cai, et al., Influence of alkali treatment on internal microstructure and tensile properties of abaca fibers, Ind. Crop. Prod. 65 (2015) 27–35.
[14] F. Pacheco-Torgal, S. Jalali, Cementitious building materials reinforced with vegetable fibres: a review, Construct. Build. Mater. 25 (2) (2011) 575–581.
[15] H. Ye, et al., Effects of cellulose, hemicellulose, and lignin on the morphology and mechanical properties of metakaolin-based geopolymer, Construct. Build. Mater. 173 (2018) 10–16.
[16] L. Yan, B. Kasal, L. Huang, A review of recent research on the use of cellulosic fibres, their fibre fabric reinforced cementitious, geo-polymer and polymer composites in civil engineering, Compos. B Eng. 92 (2016) 94–132.
[17] B. Çomak, A. Bideci, Ö. Salli Bideci, Effects of hemp fibers on characteristics of cement based mortar, Construct. Build. Mater. 169 (2018) 794–799.
[18] A.R.G. de Azevedo, et al., Natural fibers as an alternative to synthetic fibers in reinforcement of geopolymer matrices: a comparative review, Polymers 13 (15) (2021) 2493.
[19] R.A.J. Malenab, J.P.S. Ngo, M.A.B. Promentilla, Chemical treatment of waste abaca for natural fiber-reinforced geopolymer composite, Materials 10 (6) (2017) 579.
[20] L.Y. Mwaikambo, M.P. Ansell, Mechanical properties of alkali treated plant fibres and their potential as reinforcement materials. I. hemp fibres, J. Mater. Sci. 41 (8) (2006) 2483–2496.
[21] P. Maichin, et al., Effect of self-treatment process on properties of natural fiber-reinforced geopolymer composites, Mater. Manuf. Process. 35 (10) (2020) 1120–1128.
[22] J. Wei, C. Meyer, Degradation mechanisms of natural fiber in the matrix of cement composites, Cement Concr. Res. 73 (2015) 1–16.
[23] Z.N. Azwa, et al., A review on the degradability of polymeric composites based on natural fibres, Mater. Des. 47 (2013) 424–442.
[24] G. Lazorenko, et al., Effect of pre-treatment of flax tows on mechanical properties and microstructure of natural fiber reinforced geopolymer composites, Environ. Technol. Innov. 20 (2020), 101105.
[25] I. Netinger Grubeša, et al., Effect of hemp fibers on fire resistance of concrete, Construct. Build. Mater. 184 (2018) 473–484.
[26] M. Cai, et al., Effect of alkali treatment on interfacial bonding in abaca fiber-reinforced composites, Compos. Appl. Sci. Manuf. 90 (2016) 589–597.
[27] D. Sedan, et al., Mechanical properties of hemp fibre reinforced cement: influence of the fibre/matrix interaction, J. Eur. Ceram. Soc. 28 (1) (2008) 183–192.
[28] M.M. Kabir, et al., Effects of chemical treatments on hemp fibre structure, Appl. Surf. Sci. 276 (2013) 13–23.
[29] A. Rachini, et al., Comparison of the thermal degradation of natural, alkali-treated and silane-treated hemp fibers under air and an inert atmosphere, J. Appl. Polym. Sci. 112 (1) (2009) 226–234.
[30] O. Gencel, et al., Characteristics of hemp fibre reinforced foam concretes with fly ash and Taguchi optimization, Construct. Build. Mater. 294 (2021), 123607.
[31] ASTM, C348, Standard Test Method for Flexural Strength of Hydraulic-Cement Mortars, 2021.
[32] D.L.Y. Kong, J.G. Sanjayan, Effect of elevated temperatures on geopolymer paste, mortar and concrete, Cement Concr. Res. 40 (2) (2010) 334–339.
[33] M. Guerrieri, J.G. Sanjayan, Behavior of Combined Fly Ash/slag-Based Geopolymers when Exposed to High Temperatures, vol. 34, 2010, pp. 163–175, 4.
[34] RILEM, AAC 5.1, Determination of Drying Shrinkage of AAC, 1992.
[35] ASTM, C1437, Standard Test Method for Flow of Hydraulic Cement Mortar, 2007.
[36] K. Dhasindrakrishna, et al., Effect of yield stress development on the foam-stability of aerated geopolymer concrete, Cement Concr. Res. 138 (2020), 106233.
[37] Z. Li, L. Wang, X. Wang, Compressive and flexural properties of hemp fiber reinforced concrete, Fibers Polym. 5 (3) (2004) 187–197.
[38] E. Awwad, et al., Studies on fiber-reinforced concrete using industrial hemp fibers, Construct. Build. Mater. 35 (2012) 710–717.
[39] F. Matalkah, et al., Drying shrinkage of alkali activated binders cured at room temperature, Construct. Build. Mater. 201 (2019) 563–570.
[40] S. Kumar, R. Kumar, S.P. Mehrotra, Influence of granulated blast furnace slag on the reaction, structure and properties of fly ash based geopolymer, J. Mater. Sci. 45 (3) (2010) 607–615.
[41] M. Mastali, et al., Drying shrinkage in alkali-activated binders – a critical review, Construct. Build. Mater. 190 (2018) 533–550.
[42] B. Raj, et al., Mechanical and durability properties of hybrid fiber reinforced foam concrete, Construct. Build. Mater. 245 (2020), 118373.
[43] N.P. Tran, et al., A critical review on drying shrinkage mitigation strategies in cement-based materials, J. Build. Eng. 38 (2021), 102210.
[44] A. Raj, D. Sathyan, K.M. Mini, Physical and functional characteristics of foam concrete: a review, Construct. Build. Mater. 221 (2019) 787–799.

[45] Y. Tong, et al., Improving cracking and drying shrinkage properties of cement mortar by adding chemically treated luffa fibres, Construct. Build. Mater. 71 (2014) 327–333.
[46] A. Mustata, F.S.C. Mustata, Moisture Absorption and Desorption in Flax and Hemp Fibres and Yarns, Fibres & Textiles in Eastern Europe, 2013.
[47] Y. Yang, et al., Investigate on moisture absorption/desorption of shoe material containing hemp fiber, Adv. Mater. Res. 627 (2013) 49–52.
[48] I.-S. Kim, et al., Effect of internal pores formed by a superabsorbent polymer on durability and drying shrinkage of concrete specimens, Materials 14 (18) (2021) 5199.
[49] D. Ballekere Kumarappa, S. Peethamparan, M. Ngami, Autogenous shrinkage of alkali activated slag mortars: basic mechanisms and mitigation methods, Cement Concr. Res. 109 (2018) 1–9.
[50] F.d.A. Silva, et al., Physical and mechanical properties of durable sisal fiber–cement composites, Construct. Build. Mater. 24 (5) (2010) 777–785.
[51] R.D. Toledo Filho, et al., Free, restrained and drying shrinkage of cement mortar composites reinforced with vegetable fibres, Cement Concr. Compos. 27 (5) (2005) 537–546.
[52] P. Rovnaník, P. Bayer, P. Rovnaníková, Characterization of alkali activated slag paste after exposure to high temperatures, Construct. Build. Mater. 47 (2013) 1479–1487.
[53] M. Guerrieri, J. Sanjayan, F. Collins, Residual strength properties of sodium silicate alkali activated slag paste exposed to elevated temperatures, Mater. Struct. 43 (6) (2010) 765–773.